Micro-tearing modes in spherical and conventional tokamaks

S. Moradi[1], I. Pusztai[1,3], W. Guttenfelder[2], T. Fülöp[1] and A. Mollén[1]

[1]*Department of Applied Physics, Nuclear Engineering,*

Chalmers University of Technology and Euratom-VR Association, Göteborg, Sweden

[2]*Princeton Plasma Physics Laboratory, Princeton NJ 08543, USA*

[3]*Plasma Science and Fusion Center, Massachusetts*

Institute of Technology, Cambridge MA, 02139, USA

The onset and characteristics of Micro-Tearing Modes (MTM) in the core of spherical (NSTX) and conventional tokamaks (ASDEX Upgrade and JET) are studied through local linear gyrokinetic simulations with GYRO [J. Candy and E. Belli, General Atomics Report GA-A26818 (2011)]. For experimentally relevant core plasma parameters in the NSTX and ASDEX Upgrade tokamaks, in agreement with previous works, we find MTMs as the dominant linear instability. Also, for JET-like core parameters considered in our study an MTM is found as the most unstable mode. In all these plasmas, finite collisionality is needed for MTMs to become unstable and the electron temperature gradient is found to be the fundamental drive. However, a significant difference is observed in the dependence of linear growth rate of MTMs on electron temperature gradient. While it varies weakly and non-monotonically in JET and ASDEX Upgrade plasmas, in NSTX it increases with the electron temperature gradient.

I.   INTRODUCTION

In recent years, specially in view of an increasing interest in high β_e operation scenarios, such as hybrid scenarios for ITER [1, 2], the impact of electromagnetic effects on the particle and heat transport has attracted much attention. Here $\beta_e = (8\pi n_e T_e)/B_{unit}^2$, where n_e and T_e are the electron density and temperature. B_{unit} is defined as the effective field strength [3].

Recent reports have shown the significant role of electromagnetic modes such as Micro-Tearing Modes (MTMs) on the electron heat transport in the core of fusion plasmas [4–11].

It has been found that in plasmas where β_e and collisionality are sufficiently high MTMs can become the dominant instability.

The MTMs are small-scale in the radial direction, but ion-scale in the binormal direction. They are electromagnetic modes with an even parity with respect to the perturbed parallel vector potential, $\delta A_\parallel$ (referred to as *tearing parity*). In the literature two drive mechanisms for MTMs are proposed: one is the time-dependent thermal force experienced by electrons which results in a parallel current that produces magnetic field perturbations. If these perturbations then tip the field lines in the direction of an equilibrium electron temperature gradient the thermal force will increase and therefore the instability arises [12]. The second mechanism is due to a current carried by nearly trapped electrons in a boundary layer close to the trapped-passing boundary [13, 14]. Both of these mechanisms require finite electron temperature gradient and collisions. However, MTMs have been observed to arise under conditions which are not well-described by the above mechanisms [5, 10, 11, 15]. The importance of the MTM driven transport is not fully understood, and while it was shown in Ref. [6] that a sheared toroidal flow can strongly suppress the MTM turbulence and therefore reduce its related transport, in Ref. [7] the suppression of MTM transport due to an equilibrium sheared flow was shown to be less significant. Thus, a complete picture of MTM excitation and its contribution to anomalous transport is not available at present.

In the following we summarize the previous findings reported in Refs. [4, 5, 15–18]. Linear simulations for MAST [4, 5, 15], NSTX[16], and ASDEX Upgrade [18] plasmas reported that MTMs can be the dominant instabilities in the region $r/a = 0.5 - 0.8$ with the maximum growth rate at mode numbers $k_\theta \rho_s$ between $0.2 - 0.8$. Here, ρ_s is the ion sound Larmor radius, and the poloidal wave number is defined as $k_\theta = nq(r)/r$; where n is the toroidal mode number, $q(r)$ is the safety factor as a function of flux-surface label r. The electron temperature gradient is found to be the drive of the instability and a non-monotonic dependence of the growth rate on the electron-ion collisionality ν_{ei} is observed. The peak of the growth rate is observed to occur around the local experimental value of ν_{ei} for various considered radial positions. The non-monotonic dependence of the MTM growth rate on collisionality is due to the fact that, on one hand both of the driving mechanisms mentioned above require finite collisionality, and therefore stability can be expected as ν_{ei} reduces, but on the other hand, in a strongly collisional regime the strong rate of scattering of the electrons between the field lines prevents the formation of a current layer, hence MTMs are stabilized [18].

It has also been shown that by increasing the effective ion charge Z_{eff}, MTMs are desta-bilized through the Z_{eff}-dependence of the electron-ion collision frequency, see Ref. [16]. As MTMs are electromagnetic in nature a finite β_e is needed for their destabilization. For the studied discharge in Ref. [16] it is found that the β_e threshold is well below the ex-perimentally relevant β_e value and the growth rate increases moderately with increasing β_e.

Non-linear simulations confirmed the role of the electron temperature gradient as the drive of the MTM instability in spherical (NSTX, and MAST) [5, 6] as well as standard tokamaks (ASDEX Upgrade) [18]. Moreover, it has been shown that the Chirikov criterion [20] for overlapping of the magnetic islands leads to an up-shift of the electron temperature gradient threshold [6, 7, 17, 18]. Ref. [11] reported that, interestingly, linearly stable MTMs excited by non-linear coupling to zonal wave numbers can generate a significant contribution to the electron heat flux.

MTMs have also been found unstable at the plasma edge in the shallow gradient region at the pedestal top in both conventional tokamaks, such as ASDEX Upgrade [18] and JET [10], and spherical tokamaks such as NSTX [19] and MAST [9, 15]. Refs. [9, 10, 15] report that these edge MTMs exhibit some differences to the core MTMs. While similarly to the core MTMs the electron temperature gradient is an essential drive, the growth rate of unstable edge MTMs is found to be insensitive to collisionality ν_{ei}. The edge MTMs remain unstable even at $\nu_{ei} = 0$. These findings suggest the existence of some other mechanism independent of collisions as the MTM drive. An increase in density gradient which arises in the flat density region close to the pedestal top during the post-ELM pedestal recovery, is also reported to stabilize the edge MTMs [10, 15].

In the present paper we investigate the onset of the MTMs and its parametric dependence through local linear gyrokinetic simulations with the GYRO code [21], in a spherical tokamak: NSTX, and two conventional tokamaks: ASDEX Upgrade and JET. For the NSTX case we use the plasma parameters reported in Ref. [16, 17], and for the ASDEX Upgrade case we use the plasma parameters found in Ref. [18]. In the case of NSTX, the considered discharge has been part of ν^* and β dimensionless confinement scaling studies, which due to high collisionality was chosen for MTM studies. In the ASDEX-Upgrade case the considered discharge was chosen to be a well diagnosed H-Mode discharge with Type II ELMs and is characterized by strong plasma shaping and high density, with high triangularity, high

elongation, and high q_{95}. Due to the high density, the collisionality is rather large, and therefore it was chosen for MTM studies.

In the present work we re-examine these discharges with an emphasis on the parametric dependences of the MTM onset. In view of the new ITER-like wall experiments on JET, in the presented analysis we have also considered a set of JET-like parameters. These cases have been chosen since due to the high density, the collisionality in these plasmas is rather large, therefore MTMs are more likely to be destabilized. The JET-like parameters considered in this paper are not taken from any specific JET plasma discharge. The equilibria is chosen to be close to a typical JET Baseline H-mode. The main consideration for this JET-like case was to have high β and collisionality which in the literature has been shown to be suitable for finding unstable MTMs.

The remainder of the paper is organized as follows. In Sec. II the input parameters are discussed, and in Sec. III parametric dependences of the MTM onset are analyzed by presenting scans over MTM driving parameters such as collisionality, β_e and electron temperature/density scaling lengths. The conclusions are drawn in Sec. IV.

II. INPUT PARAMETERS

The plasma parameters used in our analysis are shown in table I.

TABLE I: Input parameters for densities, temperatures and their gradients.

	r/a	Z_{eff}	$n_e[10^{19}/m^3]$	$T_e[keV]$	a/L_{ne}	a/L_{Ti}	a/L_{Te}	T_i/T_e	ρ_s/a	$\nu_{ei}(a/c_s)$	$k_\theta\rho_s$
NSTX	0.6	2.91	6.0	0.44	-0.83	2.36	2.72	0.94	0.0074	1.45	0.63
AUG	0.65	3.30	7.6	0.765	0.37	2.18	3.02	1.19	0.0018	0.68	0.2
JET	0.6	3.41	7.8	1.25	0.15	2.16	2.16	1.00	0.0027	0.43	0.5

Here, $L_n = -[\partial(\ln n)/\partial r]^{-1}$, $L_T = -[\partial(\ln T)/\partial r]^{-1}$, are the density and temperature scale lengths, a is the outermost minor radius. Deuterium ions, an active impurity species denoted in table II by Z_1 (carbon for NSTX and nitrogen for ASDEX Upgrade and JET), and a passive species of impurity (tungsten unless otherwise stated) denoted in the table II by Z_2, are considered. The passive species are considered here in order to examine the impurity particle transport due to MTMs. Note that in the ASDEX Upgrade case reported

TABLE II: Input parameters for plasma ion compositions.

	Z_1	n_{Z1}/n_e	a/L_{nZ1}	Z_2	n_{Z2}/n_e
NSTX	C^{+6}	6.4%	-2.75	W^{+40}	0.02%
AUG	N^{+7}	4.8%	0.80	W^{+40}	0.02%
JET	N^{+7}	5.0%	0.14	W^{+40}	0.02%

in Ref. [18] no impurities were present and the value of a/L_{Ti} has been artificially reduced from its experimental value to eliminate the drive of Ion Temperature Gradient (ITG) modes, but here we use the experimental values.

Linear runs with GYRO include full electromagnetic effects: shear δB ($= \nabla \times \delta A_\parallel$), and compressional $\delta B_\parallel$ magnetic perturbations. Gyrokinetic electrons are assumed, and the collisions are modeled using an energy dependent Lorentz operator. Both electron-ion and electron-electron collisions are included in the electron collision frequency $\nu_e(v)$, and collisions between all ion species are accounted for. To take into account the plasma shape we have used a Miller-type local equilibrium model available in GYRO, see Refs. [3, 22]. Typical JET parameters for plasma shape and magnetic geometry are used, and the corresponding values are given in Table III. In this table, β_e is calculated in CGS units following the

TABLE III: Input parameters for plasma shape and magnetic geometry.

	$a[m]$	β_e	α_{MHD}	B_{unit}	R_0/a	$B_0[T]$	s	q	κ	δ
NSTX	0.6	0.024	0.36	0.66	1.52	0.35	1.73	1.68	1.72	0.12
AUG	0.6	0.005	0.42	2.16	3.3	2.479	1.31	2.18	1.30	0.13
JET	1.0	0.013	0.35	1.77	3.3	2.55	1.32	1.45	1.70	0.37

expression:

$$\beta_e = \frac{8\pi(n_e[10^{19}/m^3]\ 10^{-6}\ 10^{19})(T_e[keV]\ 1.6022\ 10^{-9})}{(10^4\ B_{unit}[T])^2}, \tag{1}$$

where $B_{unit} = (d\chi_t/dr)/r$ is the effective field strength with χ_t defined through the toroidal magnetic flux $2\pi\chi_t$ [3, 22], q is the safety factor, and the magnetic shear is $s = (r/q)dq/dr$. The generalized magnetohydrodynamic α parameter is defined as

$$\alpha_{MHD} = -q^2 R_0 \frac{8\pi}{B_{unit}^2} \frac{dp}{dr} c_p, \tag{2}$$

where R_0 is the effective major radius, r is the minor radius, and $p = \sum_a n_a T_a$ is the total plasma pressure. c_p is a scaling parameter which allows an artificial adjustment of α_{MHD} (affecting the magnetic curvature drift) without modifying the background gradients, as presented in Ref. [23]. Furthermore, κ is the elongation, δ is the triangularity.

Typical resolution parameters used in our linear analysis are as follows: 40 radial grid points, 12 parallel orbit mesh points ($\times 2$ signs of parallel velocity), 16 pitch angles, and 8 energies. A high radial resolution is needed since the linear instability of MTM depends on the presence of narrow resonant current layers centered on the rational surfaces. The toroidal mode numbers used here, corresponding to the ρ_s/a values in table I, are $n = 30$ for NSTX, $n = 18$ for AUG, and $n = 75$ for JET.

III. MTM INSTABILITY

Figures 1 (a,b) illustrate the linear growth rate and the real frequency of the most unstable modes in the three machines as functions of $k_\theta \rho_s$. In NSTX and JET, the MTMs (with positive real frequency in electron diamagnetic direction) are the most unstable modes in the range of $0.1 \leq k_\theta \rho_s \leq 1$, while for ASDEX Upgrade the MTMs are the most unstable modes only in the narrower wave number range $0.1 \leq k_\theta \rho_s \leq 0.3$, corresponding to longer wavelengths than those in NSTX and JET. In NSTX the MTMs remain the most unstable
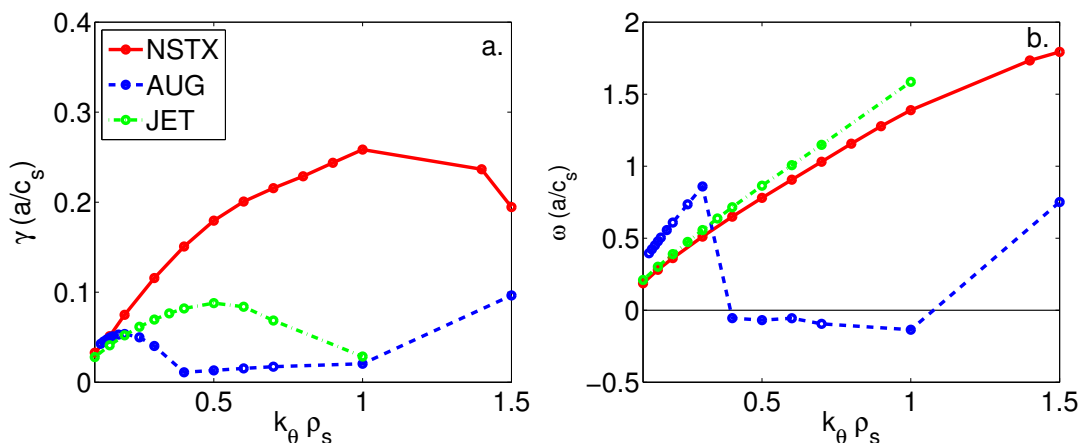

FIG. 1: Imaginary (a), and real parts (b) of eigenvalues (γ, ω_r) as functions of $k_\theta \rho_s$. Red solid lines: NSTX, blue dashed: ASDEX Upgrade, green dash-dotted: JET.

mode for the whole considered range of $k_\theta\rho_s$, but in ASDEX Upgrade an ITG mode (negative real frequency, in ion diamagnetic direction) for $0.3 < k_\theta\rho_s < 1$ and an ETG mode (positive real frequency, in electron diamagnetic direction) for $1 < k_\theta\rho_s$ are also found to be unstable. The $k_\theta\rho_s$ corresponding to the maximum growth rate varies between the different machines: in NSTX $k_\theta\rho_s \sim 1.0$, in ASDEX Upgrade $k_\theta\rho_s \sim 0.2$ and in the JET like case $k_\theta\rho_s \sim 0.5$. The normalized poloidal mode numbers for the remainder of our calculations are fixed to these values except for the NSTX case where we have chosen $k_\theta\rho_s = 0.63$ similar to the values used in Ref. [16] (see table I). Previous studies have discussed the difference in the poloidal mode number corresponding to the maximum of the unstable MTMs between the NSTX and ASDEX Upgrade cases, and it is believed to be due to characteristics of the spherical or conventional tokamaks [16, 18]. Here we find unstable MTMs with mode numbers in increasing order ASDEX Upgrade - JET - NSTX. It has been shown previously that the plasma shaping is not essential for the MTM instability [5, 15, 16, 18]. Therefore the observed trend may be a consequence of the difference in the plasma parameters (such as β_e). Further studies are needed to determine the reason for the similarities and differences in the mode numbers for maximum growth rates in various machines.

The structure of the $\delta\phi$, $\delta A_\parallel$ and $\delta B_\parallel$ eigenmodes, corresponding to the $k_\theta\rho_s$ values mentioned above are shown in figures 2 (a-f). The eigenfunctions are normalized so that $\delta A_\parallel(\xi = 0)$ is unity. The MTM signature is distinguished by the tearing parity of the $\delta A_\parallel$ eigenmodes. The NSTX case has the strongest electromagnetic character in terms of the relative amplitude of $\delta\phi$, while the "most electrostatic" mode is the AUG case. Regarding the strength of the compressional magnetic perturbations, $\delta B_\parallel$, the situation is the opposite; the less electrostatic the mode is the stronger the $\delta B_\parallel$ perturbations are. The characteristic width of the eigenmodes along the field line is similar in all three machines.

Figures 3 and 4 illustrate the normalized linear energy and particle fluxes, respectively, and the contributions to these from the $\delta\phi$, $\delta A_\parallel$ and $\delta B_\parallel$ fluctuations, as functions of $k_\theta\rho_s$ in all three machines. As seen in figures 3 (a-c), in the MTM dominated region the electron heat flux is the main channel of the energy transport, and the dominant contribution is generated by $\delta A_\parallel$ (blue dash-dotted line). In the NSTX case, see figure 3 (a), this is true for the whole considered range of $k_\theta\rho_s$. The ion heat flux generated by MTMs shown in figure 3 (d) (magenta solid line) however, is negligibly small compared to the electron heat flux. The particle fluxes generated by MTMs for electrons as seen in figure 4 (a-c), and both
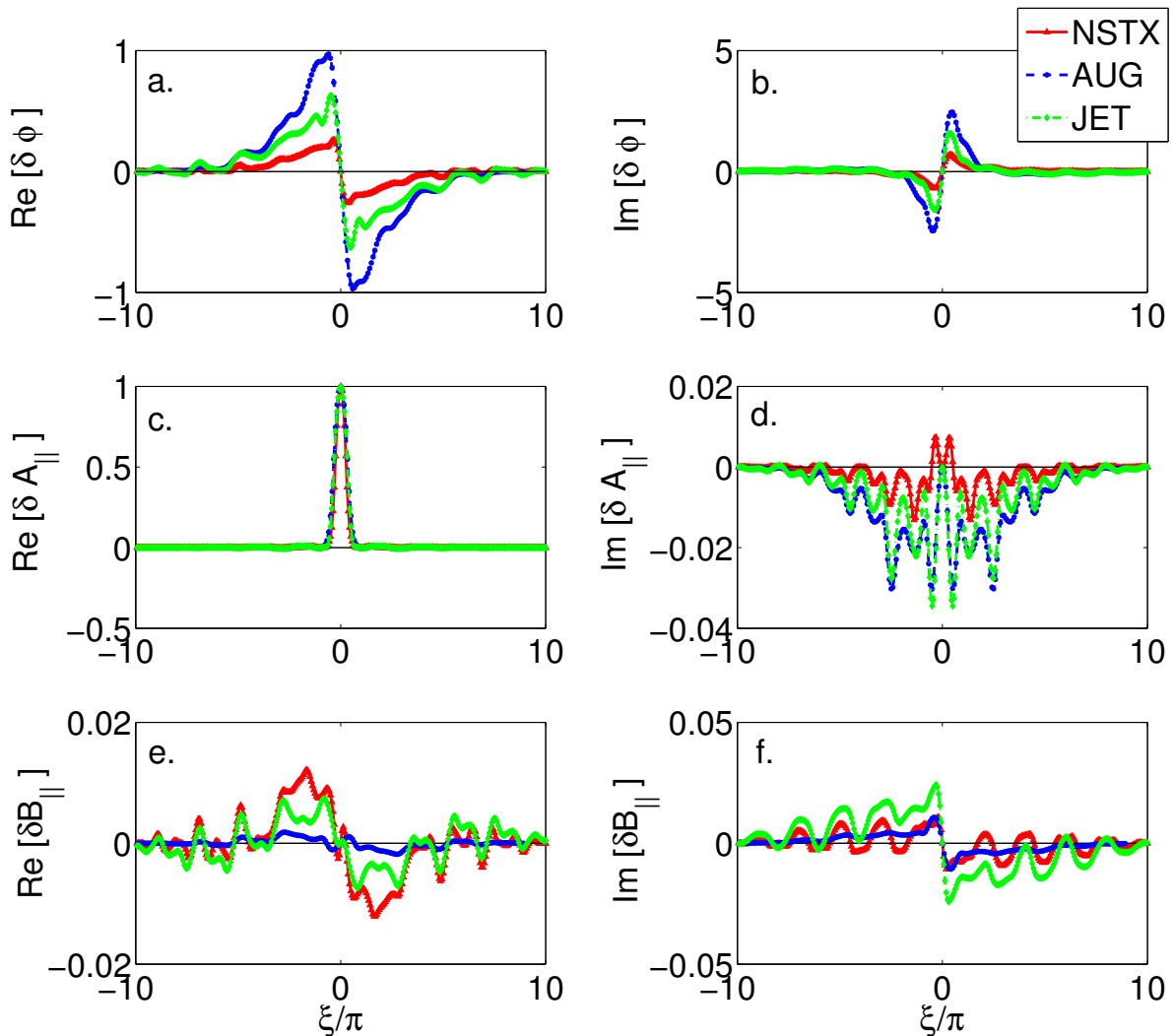
FIG. 2: Linear parallel mode structures of $\delta\phi$ (a,b), $\delta A_\parallel$ (c,d) and $\delta B_\parallel$ (e,f), as functions of the normalized extended poloidal angle ξ/π. Note that the actual radial resolution of the simulations covers $\xi/\pi = (-16, 16)$.

active and passive impurity species shown in figures 4 (d-f and g-i) are also negligible in comparison to the electron heat flux. We note, that nonlinear MTM simulations for NSTX, presented in [6, 17] also showed negligibly small particle fluxes.

In the case of ASDEX Upgrade the main contribution to electron heat flux, see figure 3 (b), is generated by the MTM instability at low $k_\theta\rho_s$, and for higher $k_\theta\rho_s$ where the most unstable mode switches to an ITG mode, the electron heat flux is significantly reduced.
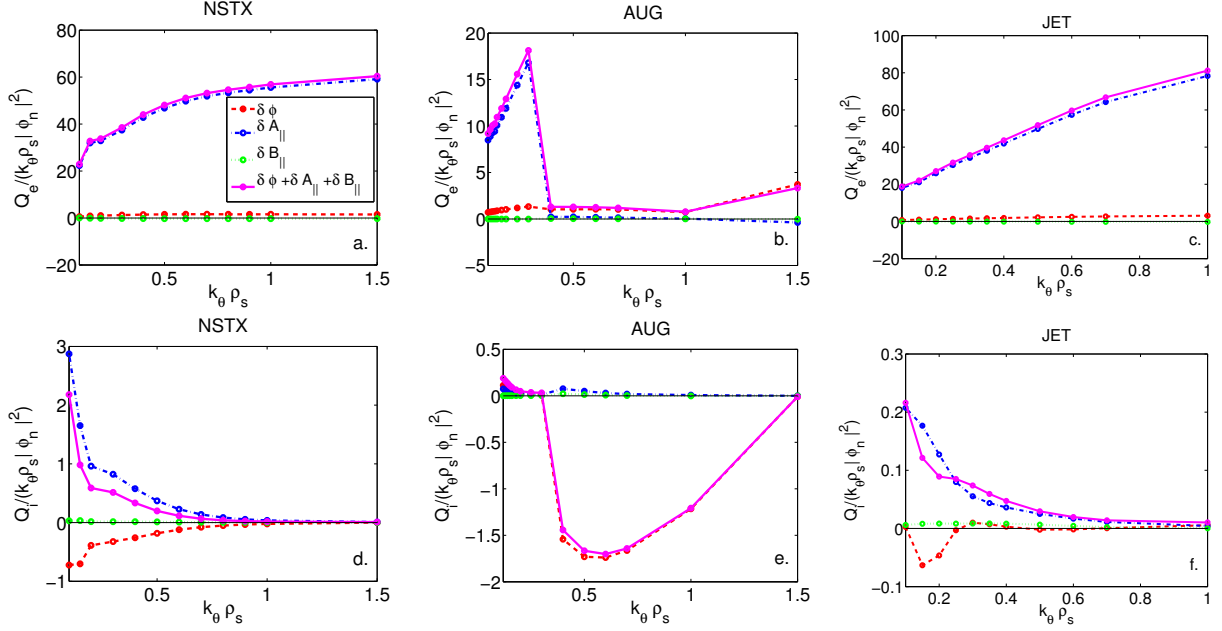
FIG. 3: Normalized linear electron (top) and ion (bottom) heat fluxes (magenta solid lines) and their contributions from $\delta\phi$ (red dashed lines), $\delta A_\parallel$ (blue dash-dotted lines), and $\delta B_\parallel$ (green dotted lines) versus $k_\theta\rho_s$ in NSTX (a, d), ASDEX Upgrade (b, e), and JET (c, f).

However, at the very high poloidal mode numbers $1 < k_\theta\rho_s$ where an ETG is the dominant instability the electron heat flux increases again. Also here, $\delta A_\parallel$ (blue dash-dotted line) generates the dominant contribution to the electron heat flux in the MTM dominated region while $\delta\phi$ (red dashed line) produces the dominant contribution to the electron heat flux in the ITG/ETG dominated regions. For the ion heat flux the main contribution comes from the higher $k_\theta\rho_s$ region where the ITG mode is the most unstable mode present with the maximum around $k_\theta\rho_s \sim 0.5$, as illustrated in figure 3 (e). The MTM and ETG contributions to the ion heat flux are significantly smaller. Also, for the electron and impurity particle fluxes, shown in figures 4 (b, e and h), the contributions from MTM and ETG are negligible compared to the contribution from the ITG.

Similar trends are observed for heat and particle transport in the JET case. Again here, in the MTM dominated region the electron heat flux, see figure 3 (c), is the main channel of transport while the ion heat flux, presented in figure 3 (f), and the particle fluxes shown in figures 4 (c, f and i) are negligibly small in comparison.

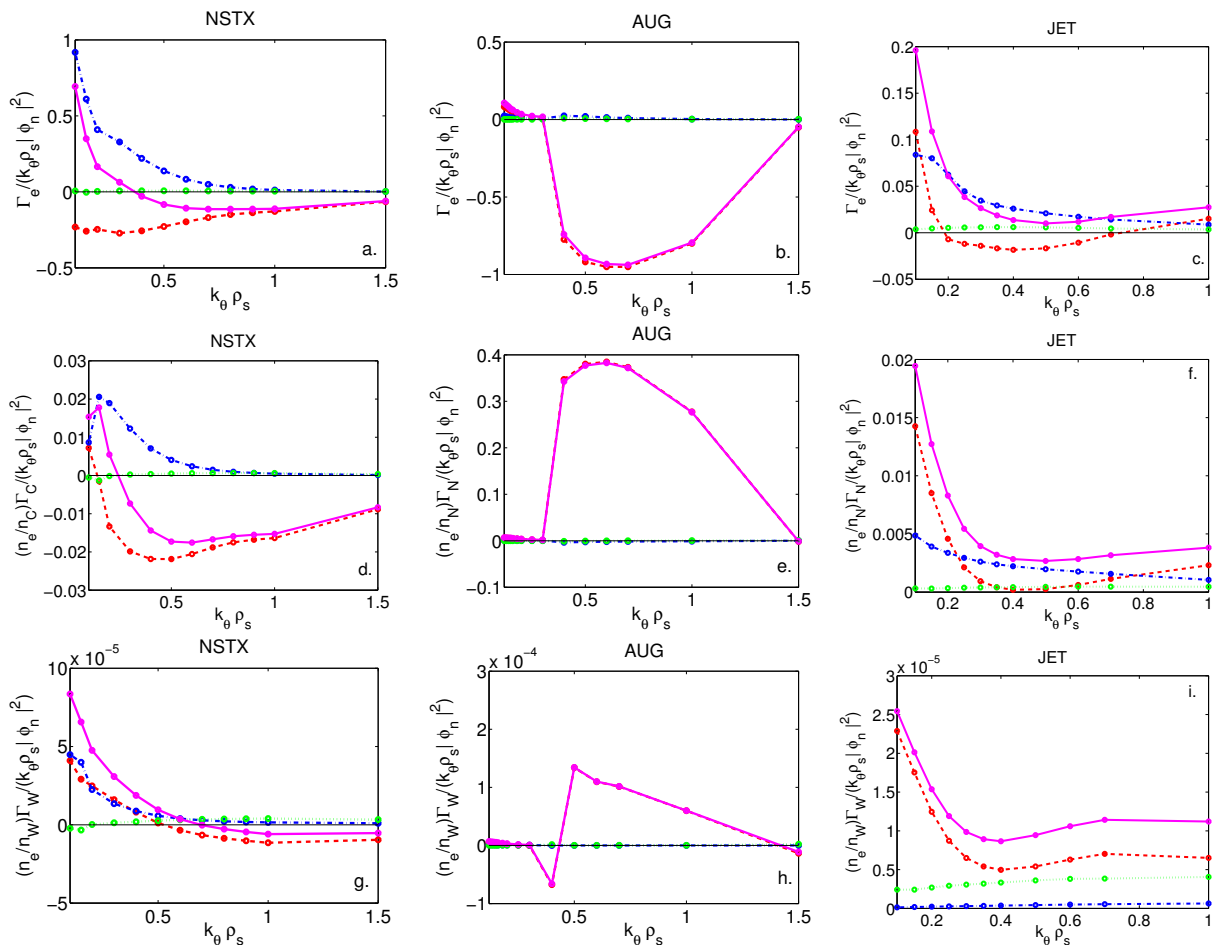Remarkably, the main ion energy fluxes (Q_i) generated by the ITG modes in the ASDEX

FIG. 4: Normalized linear particle fluxes (magenta solid lines) and their contributions from $\delta\phi$ (red dashed lines), $\delta A_\parallel$ (blue dash-dotted lines), and $\delta B_\parallel$ (green dotted lines) versus $k_\theta \rho_s$ in NSTX (a, d and g), ASDEX Upgrade (b, e and h), and JET (c, f and i).

Upgrade is found to be inward in spite of the positive ion temperature gradient, see Fig. 3 (d). However we note, that in the ASDEX Upgrade case 1) there is a high inward particle flux of main ions which might account for the inward energy flux if most of it is convective, 2) the strong positive ion energy flux carried by the nitrogen impurities almost cancel the negative energy flux of the main ions, so the total ion energy flux is close to zero.

A. Parametric dependences

Figures 5 (a,c) show the linear growth rates and the real frequencies of the unstable modes, corresponding to the fixed values of $k_\theta \rho_s$ given in table III, as functions of β_e for

the three considered machines. As seen in this figure for the experimental values of β_e (shown with vertical lines) the most unstable mode is an MTM for all three tokamaks. In NSTX, the onset of MTM is well below the experimental value of β_e and an increase in β_e above its experimental value does not increase the growth rate significantly. The same observation can be made for the JET case, while for ASDEX Upgrade, although the MTM onset is well below its experimental value, by further increasing β_e, a Kinetic-Ballooning Mode (KBM) (negative real frequency in ion direction) appears as the most unstable mode. These results show that since MTMs become unstable due to electromagnetic perturbations a finite level of β_e is needed for their onset, but around the experimental values of β_e (when there is no mode transition) no significant variation in the MTM growth rates are observed. However, the impact of an increase in β_e is important as it can increase the level of electromagnetic fluctuations which non-linearly can lead to enhanced transport. Therefore, the β_e dependence of MTMs may be stronger if non-linear effects are considered. In all these scans the value of α_{MHD} is calculated consistently with the local beta values and the density and temperature gradients.

In order to determine the effect of α_{MHD} through the curvature drift a β_e scan, similar to figure 5 (a and c), is performed where α_{MHD} is scaled to zero by setting $c_p = 0$. The corresponding results are shown in figure 6. The α_{MHD}-stabilization is not significant in the MTM regime in any of the studied plasmas. In the NSTX case there is a small α_{MHD}-stabilization only at very high β_e, see figures 6 (a,d). In the ASDEX Upgrade case, the stabilization of the KBM mode at higher β_e is clearly an α_{MHD} effect, since without it the mode is further destabilized by an increase in β_e, see the black dashed lines in figures 6 (b,e). For JET, the situation is different, as seen in figures 6 (c,f). In the electrostatic limit and at low β_e the most unstable mode is an ITG which is stabilized as β_e is increased even without α_{MHD} effects. For higher β_e the dominant mode switches to an MTM. Without α_{MHD} effects, by increasing β_e even further the MTM switches to a KBM that is further destabilized by β_e, however with the α_{MHD} effect included the KBM appears only at higher β_e (outside the plotted β_e range).

As the collisionality is suggested as an important parameter in driving the MTMs unstable, here we examine the dependence of the MTM mode characteristics on this parameter. In figures 5 (b,d) the linear growth rates and the real frequencies of the most unstable modes are shown as functions of the collision frequency ν_{ei} for the different tokamaks. For the ex-
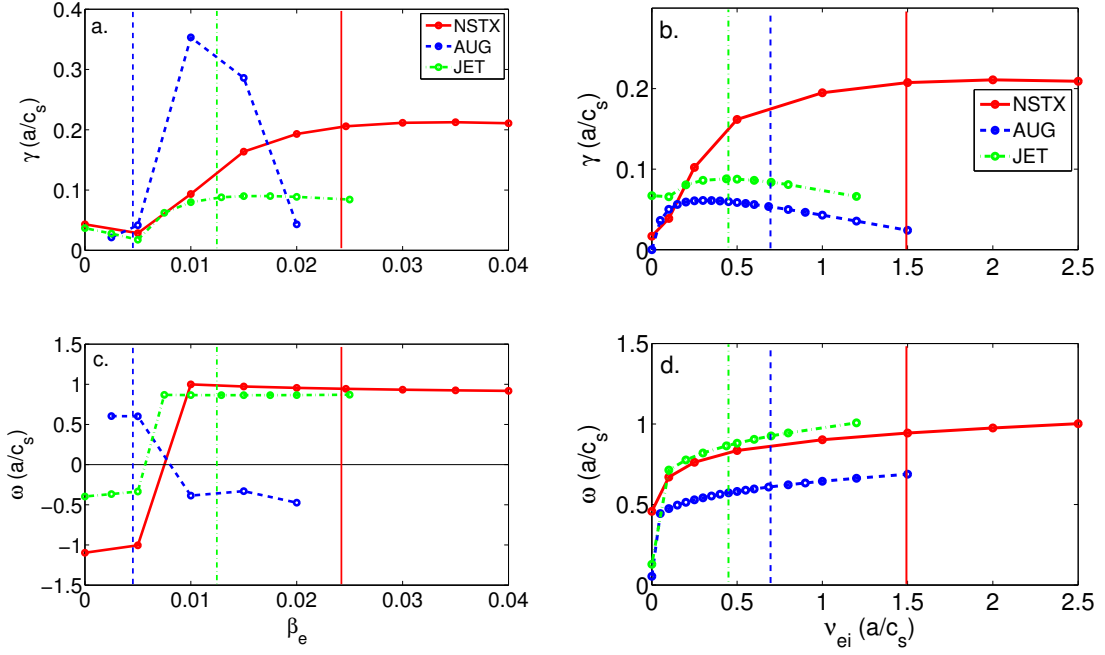
FIG. 5: Imaginary and real parts of eigenvalues (γ, ω_r) as functions of β_e (a and c), and ν_{ei} (b and d). Red solid lines: NSTX, blue dashed: ASDEX Upgrade, green dash-dotted: JET. The vertical lines represent the base parameters color coded similarly to their respective machine.
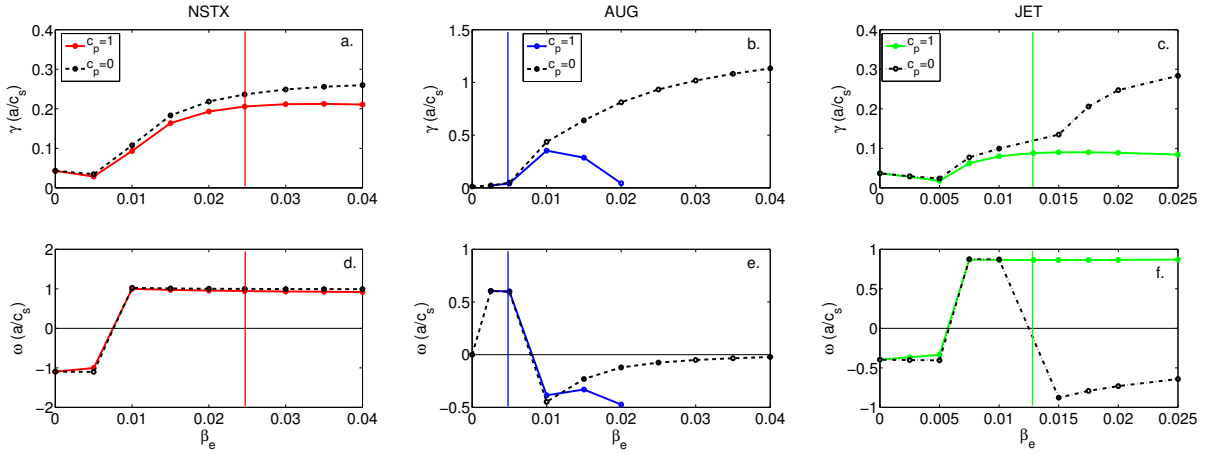

FIG. 6: Imaginary and real parts of eigenvalues (γ, ω_r) as functions of β_e for $c_p = 1$ (solid lines) and $c_p = 0$ (dashed black lines). NSTX (a and d), ASDEX Upgrade (b and e), and JET (c and f). The vertical lines represent the base parameters color coded similarly to their respective machine.

perimental values of ν_{ei} (marked with vertical lines) the most unstable mode is found to be an MTM in all the three considered tokamaks. In NSTX, the growth rate increases with collisionality as expected since collisionality is one of the instability drives [12, 13], however, a further increase in ν_{ei} above the experimental value (almost doubled) the MTM growth rate does not increase significantly. In ASDEX Upgrade the growth rate shows a decline as collisionality increases. This trend is not surprising since previous studies have shown that the growth rate of the MTM has a non-monotonic dependence on the collisionality [5–7]. As the collisionality further increases beyond the peak value, particles are very much scattered by collisions, and therefore preventing the formation of the current layer necessary for the MTMs to become unstable. Hence, as seen in figure 5 (b) we expect that this is the case for the ASDEX Upgrade case. For JET we also observe a (gentle) non-monotonic trend, and our base value of the collisionality seems to be positioned near the peak value. In all three machines no unstable MTMs were found for the collisionless case, i.e. $\nu_{ei} = 0$, and under this condition these plasmas are found to be TEM unstable. Using the eigenvalue solver method in GYRO [21] we followed the root corresponding to the MTM instability towards smaller ν_{ei}, and the mode is completely stabilized in the collisionless limit, as shown in figure 7 (a and b).

It has been shown in previous works [16] and [24] that the non-monotonic ν_{ei} dependence of MTM in NSTX and MAST is roughly explained by the slab theory regardless of whether the time dependent thermal force or trapped particle effects are responsible. In particular in the works by [25] and [26], the growth rates are found to peak around $Z_{eff}\nu_{ei}/\omega_r \sim 1-10$. In our work this seems to be true in all the considered machines where we find $Z_{eff}\nu_{ei}/\omega_r \approx 6$ in the NSTX, 1.8 in ASDEX Upgrade, and 1.74 in JET. In Ref. [15] Fig. (5b) the sensitivity of the unstable MTMs to ν_{ei} and the inverse aspect ratio $\epsilon = r/R$ is investigated, where it is shown that edge MTMs are expected to be less sensitive to collisionality and can be found unstable for $\epsilon > 0.18$ at very low collisionalities, $\nu_{ei} < 0.01$; the mode is further destabilized as ϵ is increased. In our study the ϵ varies from $0.18, 0.2$, to 0.4 in JET, ASDEX Upgrade to NSTX, respectively. However, as seen in figure 7, when ν_{ei} decreases MTMs are stabilized and a transition from MTM to TEM is obtained at $\nu_{ei} = 0$, see figure 5 (b-d).

In the literature the electron temperature gradient is suggested as one of the instability drives for MTMs [12, 13]. This has been confirmed in previous numerical studies [5–7, 10, 15]. Here we compare the role of electron temperature gradient in destabilization of the MTMs
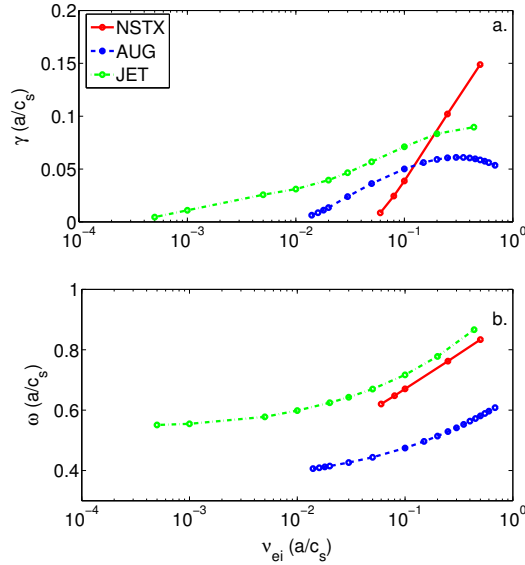
FIG. 7: Imaginary (a) and real (b) parts of eigenvalues (γ, ω_r) as functions of ν_{ei} computed by the eigenvalue solver method in GYRO. NSTX (red solid line), ASDEX Upgrade (blue dashed line), and JET (green dashed-dotted line).

between the three considered machines by performing a scan over the a/L_{Te} parameter. The results of this scan are shown in figures 8 (a,c) where the linear growth rates and the real frequencies of the most unstable modes are illustrated as functions of a/L_{Te}. As seen in this figure, a finite value of a/L_{Te} is necessary for the destabilization of the MTMs in all three machines, however a clear difference is observed in the variation of MTM growth rates with a/L_{Te} between spherical and conventional tokamaks. For the NSTX case, there is a clear increase of the MTM growth rate with an increase in a/L_{Te}, while for ASDEX Upgrade and JET the MTM growth rates show weaker and a non-monotonic dependence on a/L_{Te}. By a further increase in a/L_{Te} the most unstable mode switches from an MTM to ITG/TEM modes, corresponding to the last points in the ASDEX Upgrade and JET curves in Figs. 8 (a and c).

The a/L_{Te} threshold for MTM instabilities is observed to be well below our baseline values (indicated by vertical lines), and it is lower for JET and ASDEX Upgrade than for NSTX. The growth rate of MTMs is found to be less sensitive to electron temperature gradient for both of the conventional tokamaks than in the spherical tokamak studied here.
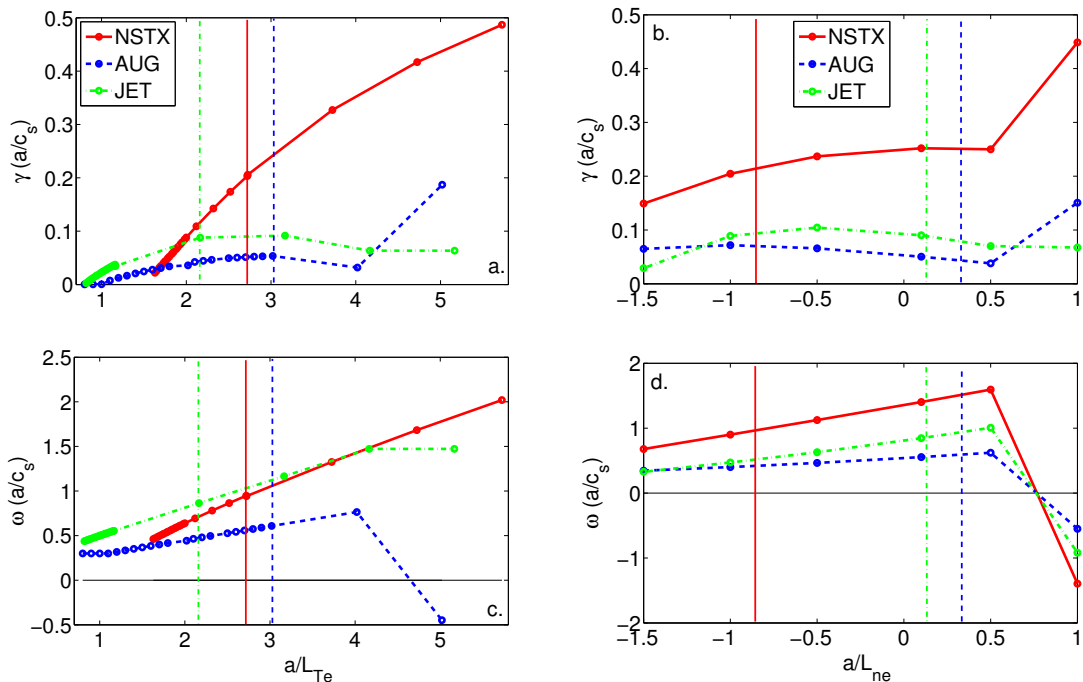
FIG. 8: Imaginary and real parts of eigenvalues (γ, ω_r) as functions of a/L_{Te} (a and c), and a/L_{ne} (b and d). Red solid lines: NSTX, blue dashed: ASDEX Upgrade, green dash-dotted: JET. The vertical lines represent the base parameters color coded similarly to their respective machine.

In order to investigate the reason for this difference we performed a similar scan over a/L_{Te} and set $c_p = 0$ to eliminate the α_{MHD} stabilization effect. The results are shown in figure 9. Without α_{MHD} stabilization the MTM still remains the most unstable mode for the baseline parameters, and as a/L_{Te} increases no significant change is observed for NSTX and ASDEX Upgrade. However, for the JET case three regions in the a/L_{Te} space can be distinguished. For low values of a/L_{Te} the MTM is the dominant instability; its growth rate increases linearly with a/L_{Te}. At $a/L_{Te} \sim 2.5$ an ITG mode, which was previously stabilized by α_{MHD} effects – see figures 8 (a,c), – becomes the dominant instability, which gradually transits to a TEM as a/L_{Te} becomes very large. Therefore, from our observations the stabilizing effect of the α_{MHD} parameter on the MTM mode is not significant, but it has an impact on the stability of ITG/TEM/KBM modes. The strong suppression of these modes therefore, allows for MTMs to remain the dominant instability for a wider range of a/L_{Te}. The weaker and non-monotonic dependence of the MTM on the electron temperature

gradient in ASDEX Upgrade and JET thus, can not be explained by this effect.
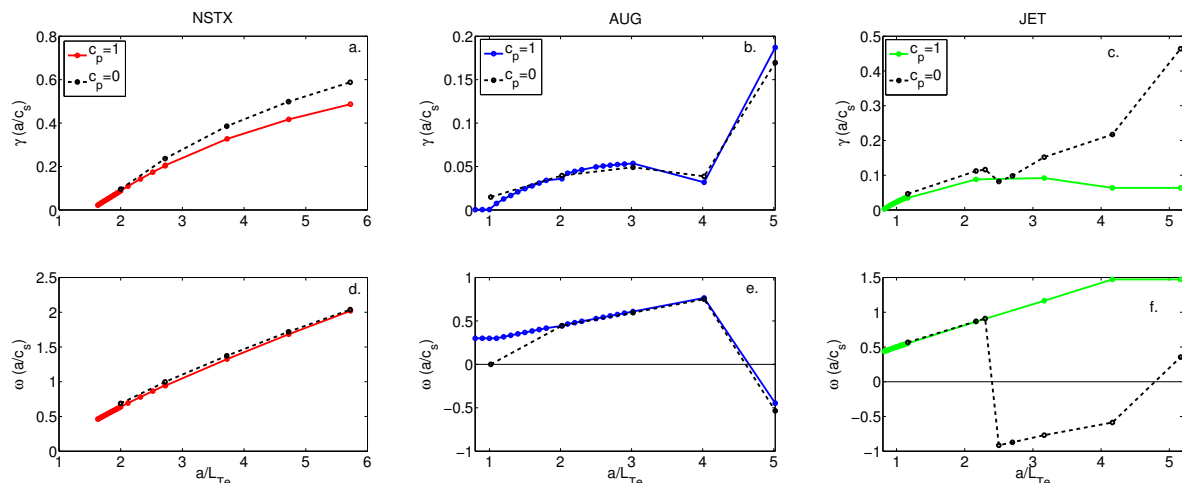

FIG. 9: Imaginary and real parts of eigenvalues (γ, ω_r) as functions of a/L_{Te} with $c_p = 1$ and $c_p = 0$. Red solid lines: NSTX, blue dashed: ASDEX Upgrade, green dash-dotted: JET.

One of the main differences between the plasma parameters in the three plasmas considered appears in the a/L_{ne} values; a strongly negative electron density gradient, corresponding to a hollow electron density profile, is observed in NSTX, while the density profiles were slightly peaked in the ASDEX Upgrade and JET plasmas. Thus, we have investigated the dependence of MTM linear growth rates on the a/L_{ne} parameter. Quasi-neutrality is enforced by slightly varying a/L_{ni} while keeping the impurity density gradients fixed to the base parameters given in table II. Figures 8 (b,d) show the linear growth rates and the real frequencies of the most unstable modes versus a/L_{ne} for the different machines. In all three machines, the MTMs linear growth rates exhibit a non-monotonic dependence on the a/L_{ne} parameter with maxima corresponding to slightly hollow electron density profiles ($a/L_{ne} \sim -0.5$) for ASDEX Upgrade and JET, but slightly peaked profile ($a/L_{ne} \sim 0.1$) for NSTX. Clearly a/L_{ne} is not a strong and necessary drive for the MTMs, as there are finite MTM growth rates in all machines at $a/L_{ne} = 0$.

In all the machines the MTM is the most unstable mode over the range of $-1.5 \leq a/L_{ne} \leq 0.5$, with a rather weak dependence on this parameter. For sufficiently high electron density gradient the dominant linear mode switches from an MTM to KBM in all plasmas. A transition from MTM to KBM with increasing a/L_{ne} has been reported previously in the

core of NSTX [16], and in MAST at the edge during the post-ELM pedestal recovery [9]. In the NSTX pedestal region of NSTX a transition from MTM to a hybrid TEM/KBM was reported in [19]. Again we examined the impact of α_{MHD} by comparing the results to corresponding simulations with $c_p = 0$ (black dashed lines in figure 10). Similar to the results of the a/L_{Te} scans shown in figure 9, the effect of the α_{MHD} parameter on the MTM mode itself is negligible, but it strongly stabilizes the KBM mode. As shown in figure 10, without α_{MHD} effects in the cases of NSTX and JET the a/L_{ne} threshold of the dominant ITG mode is reduced, but in the ASDEX Upgrade case no significant change is observed.
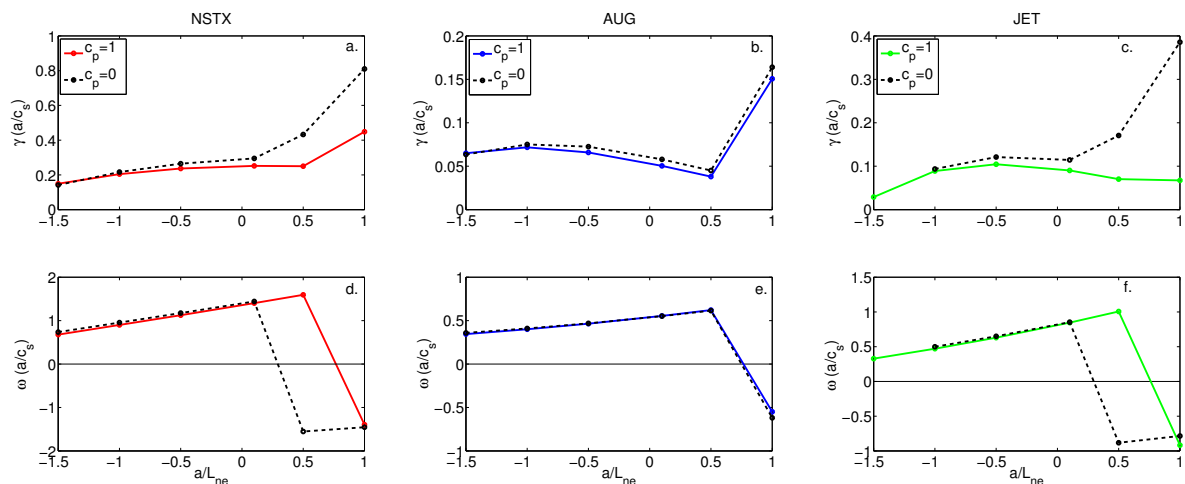

FIG. 10: Imaginary and real parts of eigenvalues (γ, ω_r) as functions of a/L_{ne} with $c_p = 1$ and $c_p = 0$. Red solid lines: NSTX, blue dashed: ASDEX Upgrade, green dash-dotted: JET.

IV.   CONCLUSIONS

We have investigated the onset and parametric dependences of the MTM instability in the core ($r/a = 0.6$) of a spherical (NSTX), and two conventional tokamaks (ASDEX Upgrade, JET). The quasilinear transport is computed using the gyrokinetic code GYRO in the flux-tube (local) limit. In confirmation with previous studies, we found that for the experimentally relevant plasma parameters the MTMs are linearly the dominant instability in NSTX and ASDEX Upgrade. Under typical JET baseline parameters considered here the MTMs are also found as the dominant linear instability. In NSTX and JET the maximum

of the MTM linear growth rate is located at higher mode numbers than that for ASDEX Upgrade. Therefore, the previously discussed idea [18], that the higher mode number MTMs are the characteristics of the spherical tokamaks, while lower mode number MTMs are the characteristics of the conventional tokamaks is not supported by our results. In agreement with previous findings we also observe that the MTM growth rate does not depend strongly on plasma geometry, and therefore the differences in the plasma parameters (such as β_e) between the different machines play the more important role in the observed mode number characteristics of the MTM growth rates.

Parametric scalings of the MTM instability in the core of these plasmas, revealed that finite levels of ν_{ei} and β_e are needed in order for MTMs to become unstable, and when unstable, they can remain the dominant instability over a wide range in ν_{ei} and β_e. Near the baseline values the linear MTM growth rate seems to be only weakly dependent on β_e, and exhibits a weak but non-monotonic dependence on collisionality, ν_{ei}. By neglecting the collisionality or β_e effects i.e. $\beta_e = 0$, or $\nu_{ei} = 0$, the ITG/TEM modes appear as the most unstable modes in all three studied machines.

A strong dependence for the growth rate of MTMs on electron temperature gradient is found in NSTX, while for ASDEX Upgrade and JET the MTM growth rate is found to be less sensitive to this parameter. The MTM growth rate significantly increases as a/L_{Te} increases in NSTX, but in ASDEX Upgrade and JET a weak and non-monotonic dependence on a/L_{Te} is found. These results indicate that while a/L_{Te} is a fundamental drive for the MTMs in these plasmas, it can contribute to the stabilization of the mode as well; this non-trivial behavior is more pronounced in the ASDEX Upgrade and JET plasmas.

Similar trends are observed in all three machines when scanning for the electron density gradient, where the MTMs linear growth rates show again a non-monotonic dependences on the a/L_{ne} parameter with peaks located in the negative a/L_{ne} region corresponding to slightly hollow electron density profiles.

We have investigated the impact of a finite α_{MHD} on the onset and characteristics of the MTM instability in various parametric scans, and we have observed that the stabilization of the α_{MHD} parameter on the MTM mode itself is not significant in all machines. However, its impact on the ITG/TEM unstable modes can result in a strong suppression of these modes allowing for the MTM to remain the dominant instability for a wider range in considered parameters, i.e. β_e, a/L_{Te} and a/L_{ne}. The non-monotonic and weaker dependence of the

MTM on the electron temperature/density gradient however, can not be explained by α_{MHD} effects.

In the studied cases the MTM drives mostly electron heat transport through $\delta A_\parallel$ fluctuations, while other transport channels and contributions from $\delta\phi$ and $\delta B_\parallel$ are significantly smaller. For the ion heat flux and particle fluxes, the transport driven by MTMs are negligible, however, if ballooning modes like ITG/TEM/KBM are also present, even as subdominant modes, these fluxes are mainly driven by these modes and therefore the overall ion heat and particle transport may not be negligible. However, these findings are based on linear analysis and further non-linear studies are needed for their confirmation.

Finally, we would like to stress that the cases which we have considered have been chosen because they were unstable to MTMs. However, particularly large aspect ratio tokamaks, being unstable to MTMs should not be considered a generic property.

Acknowledgments

Reference

[1] M. Shimada, D. J. Campbell, V. Mukhovatov, M. Fujiwara, N. Kirneva, K. Lackner, M. Nagami, V. D. Pustovitov, N. Uckan and J. Wesley International Tokamak Physics Activity Topical Group Chairs, Cochairs and Chapter Coordinators: N. Asakura, A. E. Costley, A. J. H. Donné, E. J. Doyle, A. Fasoli, C. Gormezano, Y. Gribov, O. Gruber, T. C. Hender, W. Houlberg, S. Ide, Y. Kamada, A. Leonard, B. Lipschultz, A. Loarte, K. Miyamoto, V. Mukhovatov, T. H. Osborne, A. Polevoi and A. C. C. Sips, Progress in the ITER Physics Basis Chapter 1: Overview and summary, *Nucl. Fusion* **47**, S1 (2007).

[2] D. C. McDonald, L. Laborde, J. C. DeBoo, F. Ryter, M. Brix, C. D. Challis, P. de Vries, C. Giroud, J. Hobrik, D. Howell, E. Joffrin, T. C. Luce, J. Mailloux, V. Pericoli-Ridolfini, A. C. C. Sips, K. Thomsen and JET EFDA Contributors, *Plasma Phys. Control. Fusion* **50**, 124013 (2008).

[3] R. E. Waltz and R.L. Miller, *Phys. Plasmas* **6**, 4265 (1999).

[4] D. J. Applegate, C. M. Roach, S. C. Cowley, W. D. Dorland, N. Joiner, R. J. Akers, N. J. Conway, A. R. Field, A. Patel, M. Valovic, and M. J. Walsh and EURATOM/UKAEA Fusion Association, Culham Science Centre, Abingdon, United Kingdom, *Phys. Plasmas* **11**, 5085 (2004).

[5] D. J. Applegate, C. M. Roach, J. W. Connor, S. C. Cowley, W. Dorland, R. J. Hastie and N. Joiner, *Plasma Phys. Control. Fusion* **49**, 1113 (2007).

[6] W. Guttenfelder, J. Candy, S. M. Kaye, W. M. Nevins, E. Wang, R. E. Bell, G. W. Hammett, B. P. LeBlanc, D. R. Mikkelsen and H. Yuh, *Phys. Rev. Lett.* **106**, 155004 (2011).

[7] H. Doerk, F. Jenko, M. J. Pueschel and D. R. Hatch, *Phys. Rev. Lett.* **106**, 155003 (2011).

[8] D. Told, F. Jenko, P. Xanthopoulos, L. D. Horton and E. Wolfrum, *Phys. Plasmas* **15**, 102306 (2008).

[9] D. Dickinson, C. M. Roach, S. Saarelma, R. Scannell, A. Kirk, and H. R. Wilson, *Phys. Rev. Lett.* **108**, 135002 (2012).

[10] S. Saarelma, M.N.A. Beurskens, D. Dickinson, L. Frassinetti, M.J. Leyland, C.M. Roach, EFDA-JET contributors, MHD and Gyro-kinetic stability of JET pedestals, *arXiv:1301.2919*, submitted to *Nucl. Fusion* (2013).

[11] D. R. Hatch, M. J. Pueschel, F. Jenko, W. M. Nevins, P.W. Terry, and H. Doerk, *Phys. Rev. Lett.* **108**, 235002 (2012).

[12] J. F. Drake and Y. C. Lee, *Phys. Fluids* **20**, 1341 (1977).

[13] P. J. Catto and M. N. Rosenbluth, *Phys. Fluids* **24**, 243 (1981).

[14] J. W. Connor, S. C. Cowley and R. J. Hastie, *Plasma Phys. Control. Fusion* **32**, 799 (1990).

[15] D. Dickinson, C. M. Roach, S. Saarelma, R. Scannell, A. Kirk and H. R. Wilson, *arXiv:1209.3695v1* (2012), to appear in *Plasma Phys. Control. Fusion* (2013).

[16] W. Guttenfelder, J. Candy, S. M. Nevins, R. E. Bell, G. W. Hammett, B. P. LeBlanc and H. Yuh, *Phys. Plasmas* **19**, 022506 (2012).

[17] W. Guttenfelder, J. Candy, S. M. Kaye, W. M. Nevins, E. Wang, J. Zhang, R. E. Bell, N. A.

Crocker, G. W. Hammett, B. P. LeBlanc, D. R. Mikkelsen, Y. Ren and H. Yuh, *Phys. Plasmas* **19**, 056119 (2012).

[18] H. Doerk, F. Jenko, T. Görler, D. Told, M. J. Pueschel and D. R. Hatch, *Phys. Plasmas* **19**, 055907 (2012).

[19] J. Canik, W. Guttenfelder, R. Maingi, T. Osborne, S. Kubota, Y. Ren, R. Bell, H. Kugel, B. LeBlanc and Soukhanovskii, Edge Plasma Transport and Microstability Analysis with Lithium-coated Plasma-facing Components in NSTX, submitted to *Nucl. Fusion* (January 2013), and FEC EX/P7-16, 24th IAEA Fusion Energy Conference, San Diego, USA, (2012).

[20] B. V. Chirikov, *Phys. Rep.* **52**, 263 (1979).

[21] J. Candy and R. E. Waltz, *J. Comput. Phys.*, **186**, 545 (2003).

[22] J. Candy, *Plasma Phys. Control. Fusion*, **51**, 105009 (2009).

[23] E. A. Belli and J. Candy, *Phys. Plasmas*, **17**, 112314 (2010).

[24] M. Valovič, R. Akers, M. de Bock, J. McCone, L. Garzotti, C. Michael, G. Naylor, A. Patel, C.M. Roach, R. Scannell, M. Turnyanskiy, M. Wisse, W. Guttenfelder, J. Candy and the MAST team, *Nucl. Fusion* **51**, 073045 (2011).

[25] R. D. Hazeltine, D. Dobrott, and T. S. Wang, *Phys. Fluids*, **18**, 1778 (1975).

[26] N. T. Gladd, J. F. Drake, C. L. Chang, and C. S. Liu, *Phys. Fluids* **23**, 1182 (1980).